Journal of Hydrology 590 (2020) 125334

Contents lists available at ScienceDirect

Journal of Hydrology

journal homepage: www.elsevier.com/locate/jhydrol

Research papers

Comparison of field methods for estimating evaporation from bare soil using lysimeters in a semi-arid area

Chengcheng Gong[a,b,c], Wenke Wang[a,b,*], Zaiyong Zhang[a,b], Hao Wang[a,b], Jie Luo[a,b], Philip Brunner[a,c]

[a] Key Laboratory of Subsurface Hydrology and Ecological Effects in Arid Region, Chang'an University, Ministry of Education, PR China
[b] School of Water and Environment, Chang'an University, PR China
[c] Centre for Hydrogeology and Geothermics (CHYN), University of Neuchâtel, Switzerland

ARTICLE INFO

This manuscript was handled by Huaming Guo, Editor-in-Chief, with the assistance of Mingjie Chen, Associate Editor

Keywords:
Bare soil evaporation
FAO-56 skin method
Groundwater level fluctuation method
Maximum entropy production
Phreatic evaporation
Semi-arid

ABSTRACT

Evaporation from bare soil is an important component of a catchment water balance. However, it is arguably one of the most challenging hydrological processes to estimate and measure accurately. Several approaches to estimate soil evaporation exist, but their performance for specific water table conditions remains unclear. This study investigated the performance of four commonly used approaches and several ways on how to implement them: the energy-balanced based FAO-56 method with the skin evaporation enhancement (FAO-56 skin), hydraulic methods based on groundwater level fluctuation (GLF), Darcy's law, and the maximum entropy production (MEP) method based on non-equilibrium thermodynamics theory. Three lysimeters with different water table depths were used at a research site in the Guanzhong Basin of China. The lysimeters were equipped with soil moisture probes. Water table fluctuations were also measured. The data allow us to accurately estimate evaporation rates using a water balance approach and are used to assess the performance of the analysed methods. The results show that: (1) The MEP method performed best for all water table conditions, but tends to overestimate evaporation if the water table is below the extinction depth. The extinction depth is the depth of the water table were there the contribution of groundwater to bare-soil evaporation is zero. In our case, the extinction depth was 78 cm. (2) The FAO-56 skin method underestimated evaporation where the water table was above the extinction depth, and vice versa. (3) The groundwater level fluctuation method significantly overestimated the evaporation if the specific yield was estimated using hydraulic methods. The groundwater level fluctuation method should be combined with a soil water balance, independent of water table conditions. The method can only be applied if the water table is above the extinction depth. (4) Conceptually, Darcy's law was suitable for estimating evaporation. However, the estimation of the required parameters is challenging. A good fit could only be obtained through calibration to measured evaporation rates.

1. Introduction

Evapotranspiration is one of the dominant processes in the soil–vegetation-atmosphere continuum (Lawrence et al., 2007). Brandes and Wilcox (2000) found that evapotranspiration could account for 95% of the total annual rainfall in arid regions. Despite the importance of evaporation from bare soil, Davarzani et al. (2014) reported that "Even though decades of research have improved our understanding of bare soil evaporation, many knowledge gaps still exist in the current science on how the soil water in the shallow subsurface close to the land surface interacts with the air in the atmosphere."

Reliable information on evapotranspiration is critical for irrigation scheduling, weather forecasting, and water resources management (Liu et al., 2017). Evapotranspiration also plays an important role in groundwater management. Worldwide, groundwater contributes to about 20% of freshwater consumption (Kinzelbach et al., 2003). In China, groundwater accounts for more than 60% of freshwater consumption (Ministry of Water Resources of China, 2010), and agricultural irrigation relies heavily on groundwater, especially in Northwest China (Yang et al., 2010).

Phreatic evaporation from groundwater causes soil salinity, especially in arid and semi-arid regions (Brunner et al., 2007, 2008) and diminishes water resources unproductively (Li et al., 2009; Zhang et al., 2018). Phreatic evaporation rates depend on the soil type and the depth

* Corresponding author at: School of Water and Environment, Chang'an University, Yanta Road 126, 710054, Xi'an City, Shaanxi Province, PR China.
E-mail addresses: gcc895470127@163.com (C. Gong), wenkew@chd.edu.cn (W. Wang).

https://doi.org/10.1016/j.jhydrol.2020.125334
Received 1 April 2020; Received in revised form 24 June 2020; Accepted 21 July 2020
Available online 29 August 2020

to groundwater (Brunner et al., 2008; Wang et al., 2017; Zhang et al., 2019) and therefore are difficult to determine for large spatial scales (Henderson-Sellers et al., 2003).

Many laboratory studies to estimate evaporation were conducted (Smits et al., 2012; Tran et al., 2015; Trautz et al., 2015; Wang et al., 2011). Early laboratory experiments included Veihmeyer and Brooks (1954), Gardner and Fireman (1958), Shih (1983). Hellwig (1973a), Hellwig (1973b) investigated the influences of the weather forcing, the depth of the water table, and the particle size distribution on the soil evaporation. He found that if the groundwater level was kept at the surface ground, the coarseness of the sand did not affect evaporation. However, he also pointed out that the water table depth and coarseness of the sand had a significant effect on the evaporation once the water table drops below the surface. More recent laboratory experiments mainly focused on the effect of the atmospheric conditions on actual evaporation (Lehmann et al., 2008; Shahraeeni et al., 2012; Shokri et al., 2008; Smits et al., 2012; Tran et al., 2015). However, a majority of these laboratory studies only tested one water table depth. These results are therefore difficult to apply to field conditions where the water table depth varies in space and time.

Complementary to these laboratory experiments, several field methods to estimate actual bare soil evaporation were proposed. The Bowen ratio-energy balance (BREB) is a widely applied method for estimating evaporation in the field (Bonan, 2008; Shanafield et al., 2015). BREB has the advantage of being applicable to almost any type of terrain. The BREB method is based on an energy balance and requires data such as vapor pressure gradient and temperature profiles. However, the application of the method is challenging in arid and semi-arid regions, because the gradient of vapor pressure is typically small (Shanafield et al., 2015). Isotopic profiles in the unsaturated zone have also been used to investigate evaporation, e.g. Brunner et al. (2008). Extracting isotopic profiles from the unsaturated zone are very laborious and yields point values only. In addition, numerical models are also employed to simulate evaporation from the bare soil (Bittelli et al., 2008; Li et al., 2008; Saito et al., 2006). However, the models are often based on conceptual assumptions such as homogeneity of the soil, and are therefore associated with major uncertainties.

The FAO-56 method is widely used to estimate evapotranspiration due to its straightforward implementation (Liu et al., 2017; Mutziger et al., 2005; Valipour et al., 2017). It can be applied for estimating bare soil evaporation using a crop coefficient and reference evapotranspiration (Allen et al., 1998). Rianna et al. (2018) used the FAO-56 method to estimate actual and potential bare soil evaporation over silty pyroclastic soils. Their result showed that the literature-based parameter values led to poor predictions of estimated evaporation rates. Quinn et al. (2018) evaluated the suitability of the FAO-56 method for bare sand evaporation under falling water table conditions. They found a satisfactory agreement between the field experiments and the water balance model based on the FAO-56 method. However, the experiments lasted for about 20 days only and the lysimeters were 60 cm deep. The results therefore cannot represent deep water table conditions, nor seasonal changes of atmospheric forcing.

Mutziger et al. (2005) applied a three-stage application of the FAO-56 method developed by Allen et al. (1998) to predict bare soil evaporation. The results showed that the FAO-56 approach could yield reliable results provided that site-specific information on soil parameters is available. However, Allen (2011) pointed out that the FAO-56 method underestimated evaporation when light rainfall events (less than 5 mm) occurred.

Given the practical difficulties and uncertainties of the above-mentioned approaches, alternative methods or improvement to existing approaches have been developed: (1) the semi-empirical FAO-56 method with the skin evaporation enhancement (FAO-56 skin). (2) the groundwater level fluctuation method (GLF), (3) the maximum entropy production method (MEP), and (4) Darcy's law method. The focus of this paper is on these four methods and variations of their implementation.

To overcome the issues described above with the classic FAO-56 method, a 'skin' layer enhancement to the FAO-56 evaporation method (FAO-56 skin method) was proposed by Allen (2011). FAO-56 skin method differs from the original FAO-56 method. It accommodates for wetting events which increase the soil water content near the surface. He found that the FAO-56 skin method could obtain satisfactory results compared to numerical and experimental data.

The groundwater level fluctuation method is also widely used to calculate evapotranspiration. The diurnal dynamics in evaporation rates can cause a sinusoidal response in the groundwater level. In addition to estimating evaporation rates, these variations have been used to estimate the transpiration rates of phreatophytes (Lautz, 2008). It only requires data on the fluctuation of the water table, as well as an estimation of the specific yield. However, it is very sensitive to the specific yield, which is hard to accurately obtain (Chinnasamy et al., 2018; Crosbie et al., 2005). Moreover, the specific yield can be influenced by hysteresis (Nachabe, 2002), plant activity (Logsdon et al., 2010), and antecedent soil moisture (Loheide, 2008; Loheide et al., 2005).

An approach based on the theory of maximum entropy production (MEP) was proposed by Wang and Bras (2011) and is increasingly being used (Kornejady et al., 2017). The MEP method is an unconventional, dynamic-statistical model built on non-equilibrium thermodynamics theory and the maximum entropy postulates (Dewar, 2005). The MEP has similar advantages to the BREB, for example, its robustness and the ease of implementation almost everywhere. The MEP method requires few input data, such as soil temperature of the surface ground and net radiation, and doesn't require observations of air temperature and vapor gradients. It is therefore easier to apply than the BREB approach. As for all field-based methods, a disadvantage of the MEP is the point-scale nature of its assessment.

Finally, Darcy's law is an additional method to estimate evaporation using hydraulic conductivity and the hydraulic head gradient in the soil (Qiao and Wang, 2014). Many analytical solutions based on Darcy's law have been developed for estimating steady-state evaporation, for example, Gardner (1958) proposed steady-state analytical solutions to quantify the influence of the water table on evaporation. Salvucci (1993) derived an analytic equation to calculate evaporation rates based on pressure gradients in the soil profile. However, Shokri and Salvucci (2011) pointed out that analytical solutions did not consider the discontinuity of capillary force at the drying front, thus inducing bias in the estimates. The application of Darcy's law to estimate bare soil evaporation requires high-quality data of pressure head and soil water content (Cooper et al., 1990). To the best of our knowledge, the reliability of Darcy's law to estimate evaporation has so far not been assessed outside of laboratory settings.

Comparative studies of different methods for estimating bare soil evaporation are rare. Shanafield et al. (2015) found that land surface energy balance methods, such as MEP, are especially suitable for shallow water table depths. Rianna et al. (2018) assessed the capabilities of several simplified models (for example Penman method, Penman-Monteith method, and Penman-Shuttleworth method) in estimating potential and actual evaporation for silty pyroclastic soils. They concluded that the methods performed well, provided the model parameters were calibrated using lysimeter data. The application of literature-based parameters produced biased estimates of actual evaporation.

The above mentioned comparative studies did not systematically assess the performance of the methods under different water table conditions. Given that the water table can significantly influence evaporation rates, this is an important unexplored factor. Also, few field studies integrated measurements of actual evaporation, a prerequisite to assess the performance of the different methods in absolute terms. In this study, we used data from lysimeters installed in the Guanzhong Basin of China to evaluate the performance of four approaches: the

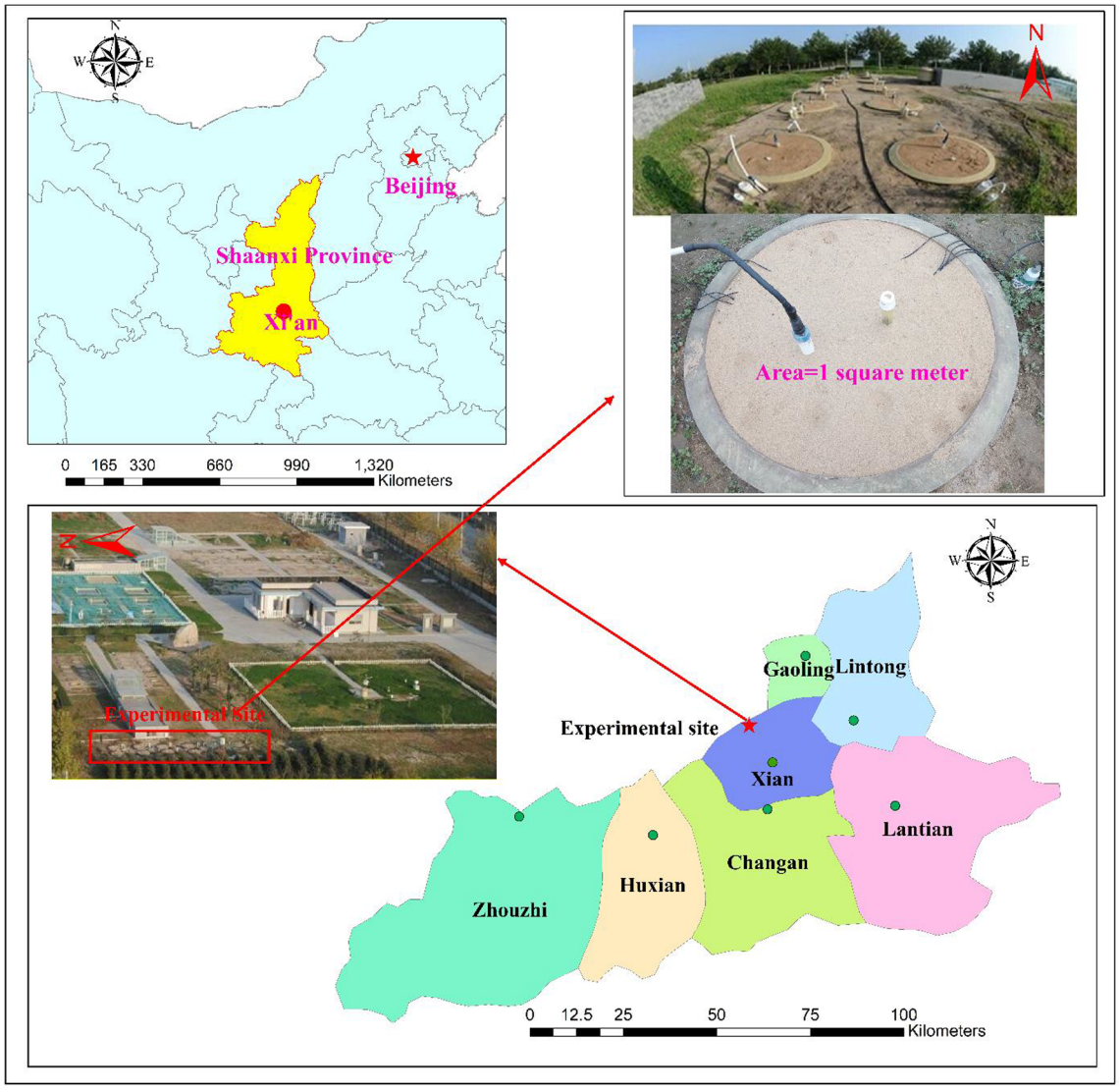

Fig. 1. Location of the field experiment in the Guanzhong Basin, Shaanxi Province, China.

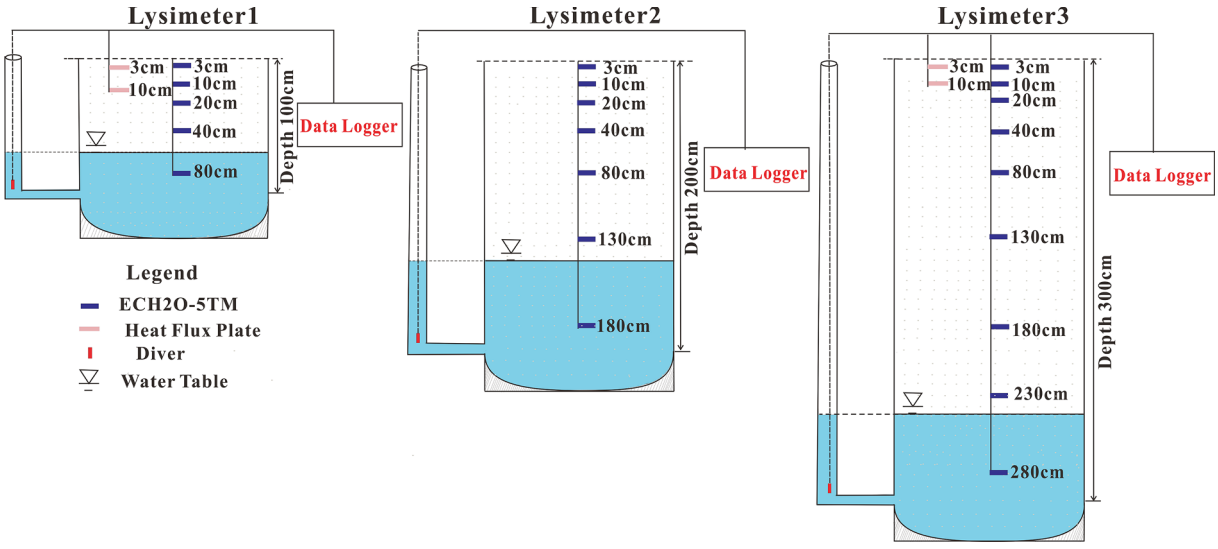

Fig. 2. Schematic diagram of the lysimeters with different water table depths.

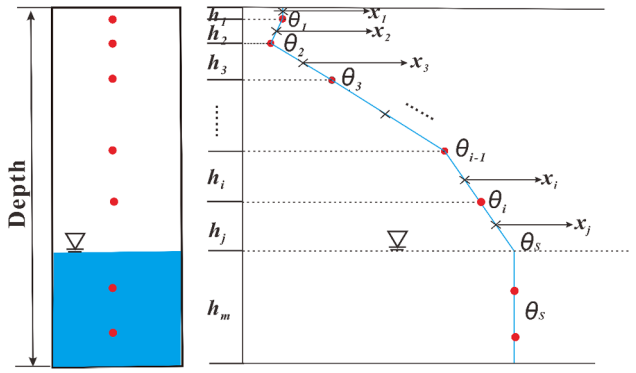

Fig. 3. Schematic diagram of water balance method to calculate evaporation. The water storage change and evaporation can be estimated by comparing the soil moisture profiles and the groundwater levels between two periods in time (five days, in this case). To calculate the water content on a specific day, the average values between two sensors (indicated with x_i in the diagram) were weighted by the distance between sensors (h_i).

FAO-56 skin method, the groundwater level fluctuation method, MEP and Darcy's law. The novelty of the study lies in the different water table depths considered. Our study includes conditions where the water table is above- as well as below the extinction depth. The extinction depth is an important factor for soil evaporation: if the water table falls under the extinction depth, no contribution from groundwater to bare soil evaporation takes place. The study also goes beyond the previous inter-comparisons studies as accurate data of evaporation rates are available through the lysimeters.

2. Materials and methods

A field experiment was carried out in the Guanzhong Basin, Shaanxi Province, China with a latitude of 34°22′14″N and a longitude of 108°54′11″E (Fig. 1). The climate is characterized by large seasonal dynamics. The mean annual air temperature was between 12 and 16 °C during the period of 56 years from 1951 to 2006 (Gao et al., 2009), the average annual actual precipitation was about 590 mm during the period of 60 years from 1951 to 2010 (Wang et al., 2018), and average potential annual evaporation was 961 mm based on 50 years of data from 1959 to 2008 (Zuo et al., 2011). Integrated cylinder-shaped lysimeters with the same surface area (1.0 m^2) and diameter (1.128 m) were installed. These lysimeters were made from glass fiber reinforced plastics with 1.2, 2.2, 3.2 m depth (Fig. 2) which prevent leakage and reduce lateral soil heat fluxes. It is very important to test different water table conditions to account for the wide range of water table depths that occur in the field.

Identical, homogenous material (sand) was used in all lysimeters. The sand was obtained from the Mu Us Desert in the northwest of China. To ensure homogenous packing, the lysimeters were filled by adding 10 cm of material at a time until the lysimeter was fully packed (Zhang et al., 2018). The initial water table depths (from the surface ground to the water table) were at approximately 0.6 m (lysimeter 1), 1.5 m (lysimeter 2), and 2.5 m (lysimeter 3) on November 1, 2016. The lower ends were sealed to prevent water leakage and infiltration from the underlying aquifer.

Soil water content and temperature were measured at 3, 10, 20, 40 and 80 cm, 3, 10, 20, 40, 80, 130 and 180 cm, and 3, 10, 20, 40, 80, 130, 180, 230 and 280 cm below the surface for lysimeter 1, lysimeter 2 and lysimeter 3 using ECH_2O-5TM (Decagon Inc, Washington State, USA), and data were automatically recorded by the EM50 (Decagon Inc, Washington State, USA). The sensors were calibrated before installation, following the protocol of Cobos and Chambers (2010). The heat fluxes were measured with heat-flux plates (Hukesflux Inc., Delft, Netherlands, Fig. 2) at the depth of 3 and 10 cm in lysimeter 1 and lysimeter 3. The data were automatically recorded by a data logger (CR-1000, Campbell Scientific, Utah, USA). Groundwater levels were recorded with a DI271 CTD-Diver (Van Essen Instruments, Delft, Netherlands). Another Diver DI500 (Van Essen Instruments, Delft, Netherlands) sensor was installed to log the air pressure for correcting the groundwater levels for atmospheric changes. A standard meteorological station was installed, and air temperature, relative humidity, precipitation, net radiation, atmospheric pressure, wind speed/direction were measured. The meteorological parameters were collected by a CR-3000 logger (Campbell Scientific, Utah, USA). All data were automatically recorded and averaged every five minutes. The lysimeters were installed in August 2014. The experiment took place from November 1, 2016 to October 31, 2017.

To obtain the soil–water characteristic curve (the relationship between soil water content and pressure head) of the soil in the lysimeter, an undisturbed soil sample was obtained at the surface of one lysimeter (lysimeter 1) using a ring knife. The soil–water characteristic curve was measured using the Ku-pF apparatus (Germany, UGT) in the laboratory. We used the van Genuchten (1980) model to fit the experimental data.

$$\begin{cases} \frac{\theta-\theta_r}{\theta_s-\theta_r} = [1+|\alpha\varphi|^n]^{-m} & \varphi < 0 \\ \theta(\varphi) = \theta_s & \varphi \geq 0 \end{cases} \quad (1)$$

where θ_s [cm^3/cm^3] and θ_r [cm^3/cm^3] are saturated and residual soil water content, respectively. φ [cm] is pressure head. α [cm^{-1}] and n [–] are two parameters, m [−] is equal to $1 - 1/n$ (Mualem, 1976).

2.1. Water balance method

This study used non-weighing lysimeters to determine evaporation using the water balance method:

$$E_a = P_e - R - \frac{dS}{dt} \quad (2)$$

where E_a [cm/d] is the actual evaporation rate, P_e [cm/d] is the effective rainfall, R [cm/d] is the surface runoff, $\frac{dS}{dt}$ [cm/d] is the total water storage change in the lysimeter. Total water storage change is composed of change in both the saturated (S_s) and the unsaturated zone (S_u), which can be calculated according to Eq. (3) (see also Fig. 3 for an illustration).

$$\frac{dS}{dt} = \frac{dS_u}{dt} + \frac{dS_s}{dt} \quad (3)$$

2.2. FAO-56 method with the skin evaporation enhancement (FAO-56 skin method)

Stage 1 evaporation (energy limited stage). In this stage, the evaporation rate is controlled by the available energy:

$$E_1 = K_{emax}\ ET_{ref} \quad (4)$$

where E_1 [cm/day] is the evaporation rate during stage 1. ET_{ref} [cm/day] is the reference evapotranspiration, typically equated to the grass reference evapotranspiration (ET_0). ET_0 was calculated by the FAO-56 Penman-Monteith equation (Allen et al., 1998). A value K_{emax} [–] of 1.2 is recommended for estimating evaporation from bare soil. The duration of stage 1 and the beginning of stage 2 can range from one to several days, depending on the amount of water that infiltrated and soil properties such as the albedo, porosity, and the hydraulic conductivity.

Stage 2 evaporation (falling rate stage or soil limited stage). The rate of evaporation is controlled by the moisture content in the upper soil layer. Evaporation is thus limited by both soil hydraulics and $K_{emax}\ ET_{ref}$ (Allen, 2011). The original FAO-56 model for E_2 was:

$$E_2 = K_e\ ET_{ref} \quad (5)$$

where K_e [−] is the evaporation coefficient.

$$K_e = K_r(K_{cmax} - K_s K_{cb}) \tag{6}$$

such that

$$K_e \le f_{ew}\ K_{cmax} \tag{7}$$

where the dual K_c model estimates ET as:

$$ET = (K_s K_{cb} + K_e) ET_{ref} \tag{8}$$

where K_e [–] is the soil evaporation coefficient, K_{cb} [–] is the basal crop coefficient, K_{cmax} is the maximum value of K_c[−] depending on the amount of rain or irrigation per wetting event, K_s [–] is a reduction coefficient to account for reduced transpiration under soil water shortage (0 for bare soil) and K_r [–] is a dimensionless evaporation reduction coefficient [0–1]. The parameter f_{ew} [–] represents the fraction of soil surface from which most of the evaporation occurs. With the skin evaporation enhancement K_e [–] is reformulated for bare soil only, i.e. in the absence of vegetation:

$$K_e = f_w[F_t + (1 - F_t)K_r]K_{emax} \tag{9}$$

$$F_t = \min\left(\frac{REW - D_{REW_{i-1}}}{K_{emax} ET_{ref}},\ 1.0\right) \tag{10}$$

where $D_{REW_{i-1}}$ [cm] is the depletion of the skin layer at the end of the previous time step (day or hour), REW [cm] is readily evaporable water, which is the maximum depth of water that can be evaporated from the topsoil layer without restriction during stage 1 (Allen et al., 1998). f_w [–] is the fraction of the wetted surface.

$$0.0 \le D_{REW_i} = D_{REW_{i-1}} - \left[(1 - f_b)\left(P_i - RO_i + \frac{I_i}{f_w}\right) + f_b\left(P_{i+1} - RO_{i+1} + \frac{I_{i+1}}{f_w}\right)\right] C_{eff} + \frac{E_i}{f_{ew}} \le REW \tag{11}$$

$$REW = \min\left[\left(2 + \frac{TEW}{3}\right),\ 0.8TEW\right] \tag{12}$$

$$TEW = 1000\,(\theta_{FC} - 0.5\theta_{WP}) z_e \tag{13}$$

where TEW [mm] is the total amount of evaporated water, which is equal to the maximum depth of water which can be evaporated from the surface soil layer when the layer has been initially completely wetted. f_b [–] is the fraction of the precipitation and irrigation during a time step [hour or day] that contributes to evaporation during that same timestep. θ_{FC} [cm^3/cm^3] is field capacity, θ_{WP} [cm^3/cm^3] is the wilting point. z_e [cm] is the effective depth of soil, with a recommended value of 0.10–0.15 m by FAO-56. P_i [cm] is precipitation and RO_i [cm] is runoff during timestep i. I_i [cm] is the irrigation depth in timestep i that infiltrates the soil. E_i [mm] is evaporation during timestep i. C_{eff} [-] is a spatial infiltration efficiency factor that represents the effectiveness of the skin layer in capturing precipitation and irrigation additions. C_{eff} is estimated as

$$C_{eff} = \min\left\{\left[C_0 + C_1\left(1 - \frac{D_{e_{i-1}}}{TEW}\right)\right],\ 1.0\right\} \tag{14}$$

C_{eff} is expressed as a fraction (0–1), $D_{e_{i-1}}$ [cm] is the depletion depth through the total evaporation, C_0 and C_1 are the fitted offset and slope of the function (Allen, 2011).

Mutziger et al. (2005) evaluated three different methods to obtain the soil parameters: (1) general soil parameters from FAO-56 (see Table 7 in Mutziger et al. (2005)); (2) the application of literature values obtained in case studies and (3) the calibrated soil parameters to obtain the best fit between the measured and estimated rates of evaporation. This requires, however, observations of evaporation, which in most cases are not available. Therefore, we used the most commonly used approach and based our estimates on reported literature values, specifically Suleiman et al. (2007) who suggested a TEW of 15 mm, REW of 6 mm, z_e of 0.15 m, θ_{FC} of 0.12 cm^3/cm^3, and θ_{WP} of 0.04 cm^3/cm^3 for sandy soils, as is the case for our study.

2.3. Maximum entropy production model of evaporation

The MEP method proposed by Wang and Bras (2011) only requires net radiation R_n [W/m^2], surface temperature T_s [K], and specific humidity q_s [kg/kg] to obtain the sensible heat flux H [W/m^2], the ground heat flux G [W/m^2], and evaporation rates E [W/m^2] simultaneously.

$$E + H + G = R_n \tag{15}$$

$$G = \frac{B(\sigma) I_s}{\sigma I_0} H\,|H|^{-\frac{1}{6}} \tag{16}$$

$$E = B(\sigma) H \tag{17}$$

where I_s [J m^{-2} K^{-1} $s^{-1/2}$] and I_0 [J m^{-2} K^{-1} $s^{-1/2}$] are the thermal and apparent thermal inertia of the soil and air respectively. $B(\sigma)$ [–] is the reciprocal of the Bowen ratio:

$$B(\sigma) = 6\left(\sqrt{1 + \frac{11}{36}\sigma} - 1\right) \tag{18}$$

The dimensionless parameter σ [–] is characterizing the phase-change related state of the evaporating surface and can be calculated using the following equation:

$$\sigma(T_s, q_s) = \left(\frac{\theta}{\theta_s}\right)^{\beta} \frac{\lambda^2 q_s}{c_p R_v T_s^2} \tag{19}$$

c_p [J kg^{-1} K^{-1}] is the specific heat of the air under constant pressure (1004 J kg^{-1} K^{-1}), λ [J/kg] is the vaporization heat of liquid water (2500000 J/kg), R_v [J kg^{-1} K^{-1}] is the gas constant for water vapor (461.5 J kg^{-1} K^{-1}). θ [cm^3/cm^3] is the soil moisture content near the surface ground, θ_s [cm^3/cm^3] is the saturated soil moisture content. T_s [K] is the near-surface ground temperature (below surface ground 3 cm). β [–] is an empirical parameter dependent on soil texture. Deardorff (1977) suggested a value of 1.0. Alternatively, β [–] also can be obtained using Eq. (19) by fitting the results of MEP to the observed heat or evaporation fluxes (Huang and Wang, 2016; Li et al., 2020). This requires either measurements of the heat flux or measurements of evaporation from e.g. a lysimeter. q_s [kg/kg] is the specific humidity. In this study, the specific humidity was approximated as the air specific humidity near the soil surface, which was calculated using the Clausius-Clapeyron equation with surface temperature and relative humidity measured near the soil surface (Alves et al., 2019; Hajji et al., 2018):

$$E_s = 6.1121 * \exp\left(\left(18.678 - \left(\frac{T_a}{234.5}\right)\right) * (T_a/(257.14 + T_a))\right) \tag{20}$$

$$E_{atm} = (RH * E_s)/100.0 \tag{21}$$

if $E_{atm} < E_s$,

$$q_s = \frac{0.622 * E_{atm}}{P - E_{atm} * (1 - 0.622)} \tag{22}$$

If $E_{atm} \ge E_s$,

$$q_s = \frac{0.622 * E_s}{P - E_s * (1 - 0.622)} \tag{23}$$

In this equation, P [kpa] is the air pressure, T_a [°C] is the air temperature, RH [%] is the relative humidity, E_s [hpa] is the saturation water vapor pressure, and E_{atm} [hpa] is the water vapor pressure.

2.4. Groundwater level fluctuation method

Evaporation can be estimated using diurnal patterns of groundwater level change at low cost (Cheng et al., 2013). Groundwater level

fluctuations result from changing evaporation rates during the course of the day. The groundwater fluctuation method is a daily water balance, with recharge by rainfall and discharge by the evaporative flux (Shanafield et al., 2015). This is well suited to our lysimeters, as the daily groundwater level variations are controlled only by rainfall and evaporation. The following formula to calculate the evaporation E [cm/day] was used:

$$E = S_y \frac{dh}{dt} \tag{24}$$

where S_y [–] is the specific yield, and $\frac{dh}{dt}$ [cm/day] is the decline rate of the groundwater table. The specific yield is an important parameter for the calculation of groundwater recharge or evaporation using the water table fluctuation method (Chinnasamy et al., 2018; Hill and Durchholz, 2015; Shah and Ross, 2009). The specific yield is defined as the volume of water that can be released from storage per unit surface area of porous material per unit decline of the water table (Freeze and Cherry, 1979). It can be expressed with the following equation (25):

$$S_y = \frac{V_w}{A\Delta z} \tag{25}$$

In this equation, V_w [cm^3] is the volume of water that can be released from storage, A [cm^2] is the surface area of the lysimeter, Δz [cm] is the decline of the water table. To obtain an estimation of the specific yield, we used two methods: a pumping test, and a water balance method (Sophocleous, 1991) considering soil moisture changes in the unsaturated zone- as opposed to the pumping test which simply considers changes of the vertical extent of the saturated zone. Pumping tests were carried out using a peristaltic pump to extract water at a constant rate (2000 ml/min) in all three lysimeters. The pump inlet was placed at the bottom of the lysimeters. Moreover, we measured the volume of the water at the outlet in order to get an accurate measurement of volume of abstracted water. The test was carried out during the period from April 28, 2018 to May 12, 2018. To avoid the influence of precipitation and evaporation during the pumping tests, the surface of the lysimeters were covered by plastic. The groundwater table fluctuation method using the specific yield based on the pumping test is subsequently called GLF-G1 method.

An alternative approach to estimating the specific yield was proposed by Sophocleous (1991). This "hybrid water-fluctuation method" combines observations of soil water content along the profile to estimate recharge. By combining groundwater level rises with precipitation and by associating the estimation of recharge using soil water balance with the subsequent water table rise, a specific yield can be estimated. The groundwater level fluctuation method using the specific yield based on the hybrid water-fluctuation approach is subsequently called GLF-G2 method.

2.5. Darcy's law method

Darcy's law (downward positive) can be expressed by equation (26):

$$q = -K(\varphi)\frac{\partial H}{\partial z} \tag{26}$$

$$H = \varphi + z \tag{27}$$

$$K(\varphi) = K_s(1 - (\alpha|\varphi|)^{n-1}[1 + (\alpha|\varphi|)^n]^{-m})^2[1 + (\alpha|\varphi|)^n]^{\left(-\frac{m}{2}\right)} \tag{28}$$

where q [cm/day] is the volumetric water flux through the soil-atmosphere interface (corresponding to evaporation if the flux is upward-moving), $K(\varphi)$ [cm/day] is the hydraulic conductivity for unsaturated conditions according to e.g. the van Genuchten (1980) model, K_S [cm/day] is the saturated hydraulic conductivity, z [cm] is the axis of coordinates and coordinate origin is on the surface, and H [cm] is the total head. φ [cm] is the pressure head which can be calculated based on soil moisture measurements and the soil water retention (Eq. (1)).

The vertical upward flux close to the soil represents evaporation (Stephens and Knowlton Jr, 1986). We used a numerical approach to solve Darcy's law. This required a vertical discretization. There are different methods to calculate the effective hydraulic conductivity between two nodes, for example, a harmonic average, arithmetic average, geometric average or a weighted average. We applied the geometric average method (Chen et al., 2018) to calculate the unsaturated hydraulic conductivity. In a discretized scheme, the vertical flux between two nodes was thus calculated as follows:

$$q_{z_i} = \sqrt{K_n K_{n-1}}\left(\frac{H_{n-1} - H_n}{z_{i-1} - z_i}\right) \tag{29}$$

where K_n and K_{n-1} are the unsaturated hydraulic conductivities below and above the node z_i, respectively. H_n and H_{n-1} are the hydraulic heads below and above the node z_i, respectively.

Two different implementations were tested. We first used the soil parameters based on the laboratory analysis (see Table 2). To further explore the conceptual suitability of this approach, to reproduce evaporation dynamics, we calibrated the van Genuchten parameters by minimizing the root-mean-square error between the cumulative evaporation of Darcy's law and actual cumulative evaporation.

3. Results

3.1. Soil properties and parameters

The particle size distribution is shown in Table 1, and the estimated van Genuchten parameters in Table 2. The saturated hydraulic conductivity, obtained using a permeameter, was 450 cm/day.

3.2. Air temperature, rainfall and water table depth

The daily averaged values of air temperature, rainfall and water table depth are displayed in Fig. 4. A total of 96 rainfall events with an average value of 0.65 cm occurred during the experimental period. Daily rainfall rates less than 2 cm are common. Rainfall mainly occurred in April, August, September, and October (Fig. 4). The average daily air temperature can be seen in Fig. 4 during the experimental period.

The fluctuations of the water table depth for every lysimeter are shown in Fig. 4*b*. The extinction depth can be graphically identified in Fig. 4*b*, which was 78 cm. The water table cannot drop below this level, despite the evaporative forcing at the soil surface. In this case, evaporation is depleting storage from the unsaturated zone. The water table in lysimeter 1 is above the extinction depth throughout the experiment. Water table depths in lysimeter 2 and 3 are below the extinction depth before June 4, 2017 and before October 9, 2017, respectively. The dynamics of the groundwater level were quite different for each lysimeter. The distributions of the water table depth could be divided into two periods: the first period from November 1, 2016 to March 11, 2017 with little change of the water table and a second period from March 12 to October 31 where the water table increased rapidly, except for lysimeter 1. The water table depth of lysimeter 2 and 3 increased rapidly with rates of 0.48 and 0.76 cm/day in this second period. Because the vadose zone was shallow in lysimeter 1, a large portion of infiltration was lost to evaporation.

Net radiation kept stable from November to January 2017. It subsequently increased from February to June and decreased from July to October (Fig. 4*c*). Reference evaporation (ET_0) is shown in Fig. 4*d*. The

Table 1
Particle size of the soil in the lysimeter.

Particle size [mm]	0.075	0.075–0.25	0.25–0.5	0.5–1
Composition [%]	2.5	73.6	23.4	0.5

Table 2
The van-Genuchten parameters.

θ_s [cm^3/cm^3]	θ_r [cm^3/cm^3]	α [cm^{-1}]	n [−]	RMSE	R^2
0.32	0.022	0.022	4.14	8.2E−12	0.999

variations were similar to net radiation.

3.3. Calculation of actual evaporation and intercomparison of different methods

The cumulative monthly evaporation rates are presented in Fig. 5 for all methods. The water balance method provides actual soil evaporation rates (Fig. 5). The cumulative actual evaporation during the experimental period was 44.1 cm for lysimeter 1, 35.8 cm for lysimeter 2, 22.7 cm for lysimeter 3. Besides relative humidity, wind speed, radiation, the actual evaporation rates can, to a certain extent, be explained with air temperature. For example, evaporation rates were low during winter and as the air temperature increased, evaporation rates increased, too. Clearly, air temperature alone cannot explain the evaporation dynamics, the influence of the water table (Fig. 4*b*) on actual evaporation needs to be examined, too.

Evaporation rates in lysimeter 2 and 3 were basically the same from November 2016 to May 2017, while evaporation in lysimeter 1 and 2 were almost identical from June to October 2017 (Fig. 5). A reasonable suggestion is to relate these different dynamics to the water table. The position of the water table has a large influence to what extent the evaporation is controlled by the available energy (atmosphere-controlled) or the soil properties. In this context, evaporation can be divided into two distinct stages for bare soil (Allen et al., 2005; Ritchie and Johson, 1990), see section 2.2. The first stage is an "energy limited" stage, and the second stage is a "falling rate" or "soil stage" (Allen et al., 2005). A comparison between potential and actual evaporation can indicate at which stage the system is. This is illustrated with an example in Fig. 6 covering a period of 20 days. Initially, after a strong rainfall event, the actual and potential evapotranspiration were nearly identical, indicating atmospherically controlled conditions (stage 1). As the water evaporates, the soil properties and the soil water content began to control the evaporation processes. Flammini et al. (2018) proposed a simple procedure to identify the first two stages of the evaporation process which we employed here, too. If the soil water content drops below the field capacity, the system is considered to be in stage 2. This analysis was carried out for all lysimeters over the entire period. We found that for the conditions analyzed here, only for 17% of the time for lysimeter 1, 10% for lysimeter 2, and 0% for lysimeter 3 the systems were controlled by the atmosphere. For the remaining time, the water availability and the soil properties controlled the evaporation rates.

3.4. Comparison of actual evaporation with the FAO-56 skin method

The values of monthly cumulative evaporation are compared in Fig. 7 with the FAO-56 skin method.

The cumulative amount of evaporation during the experimental period using the FAO-56 skin method was 34.6 cm. On the annual scale,

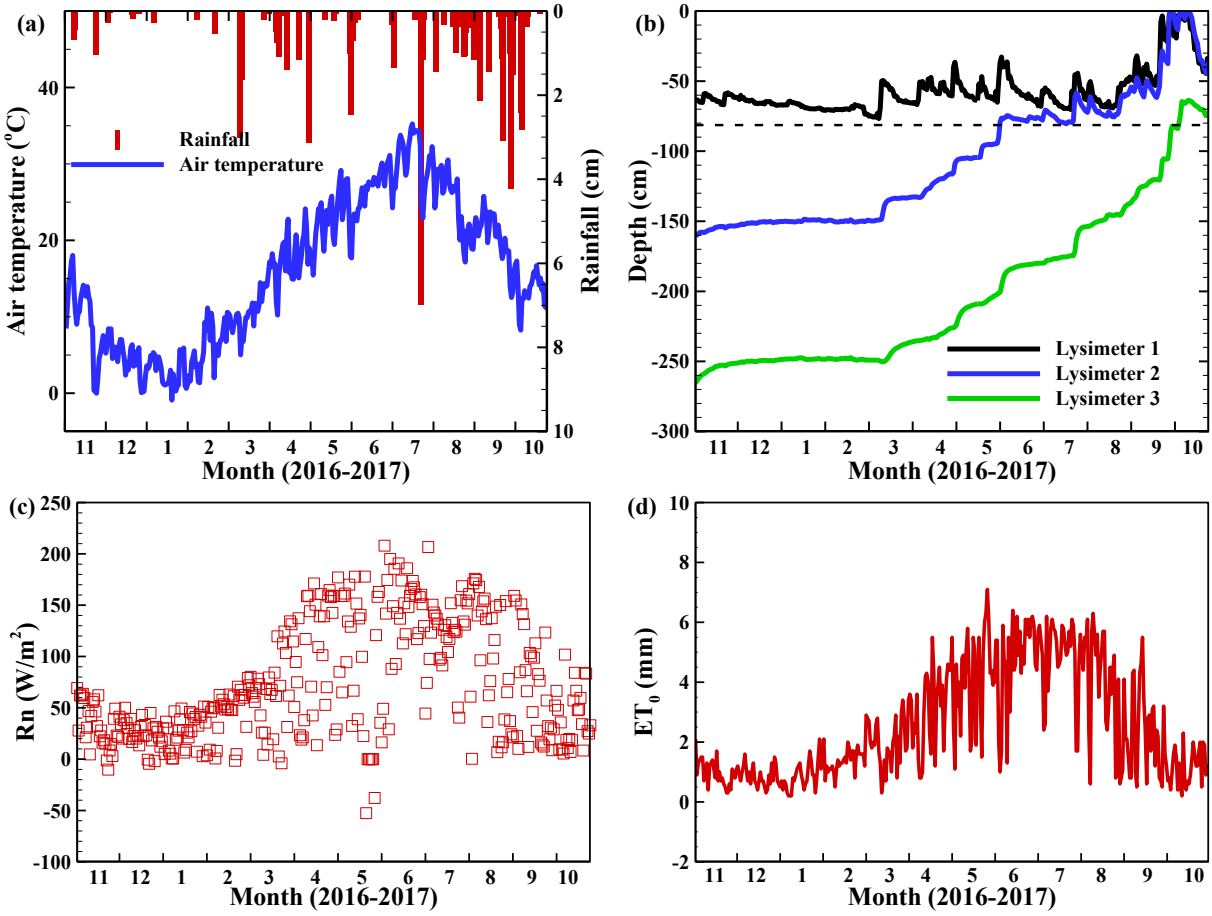

Fig. 4. (a) Rainfall and air temperature; (b) water table depth in each lysimeter. (The dashed line represents the extinction depth. If the water table depth falls below this depth, evaporation from the water table is no longer occurring); (c) net radiation and (d) reference evaporation (ET_0) estimated using the Penman-Monteith equation.

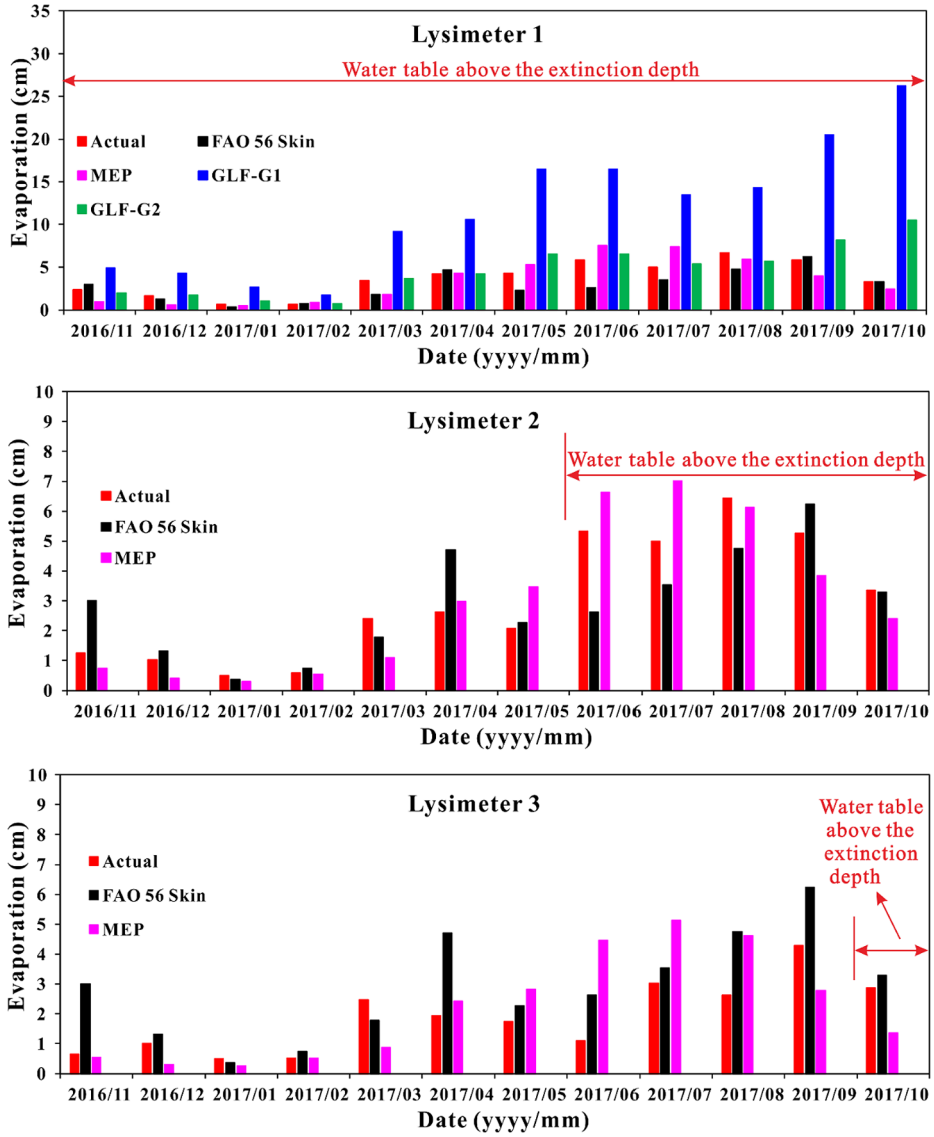

Fig. 5. Comparison of monthly evaporation rates for the methods. GLF stands for the groundwater level fluctuation method. In GLF-G1, the specific yield was obtained by a pumping test, GLF-G2 uses an estimate of the specific yield based on the approach of Sophocleous (1991). During the experimental period, the groundwater levels in lysimeter 2 and 3 increased, therefore the GLF method can only be applied to lysimeter 1. Evaporation based on Darcy's law method is not shown in this graph (see Section 3.7).

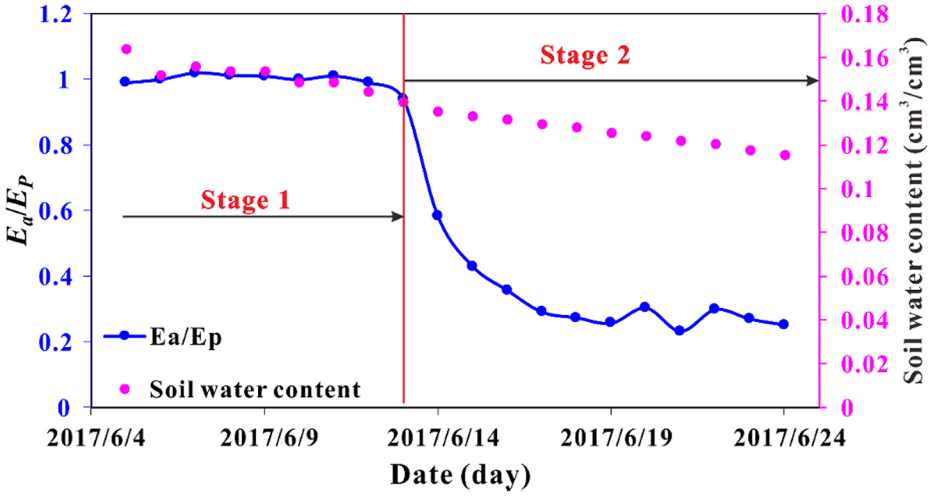

Fig. 6. Example of the identification of the different stages of evaporation. In Stage 1, energy limits the evaporation rates. The boundary between stage 1 and 2 can be identified through the soil water content in the topsoil (measured at 3 cm in our case). Once stage 2 is reached, the evaporation rate rapidly declines in comparison to the potential evaporation rate.

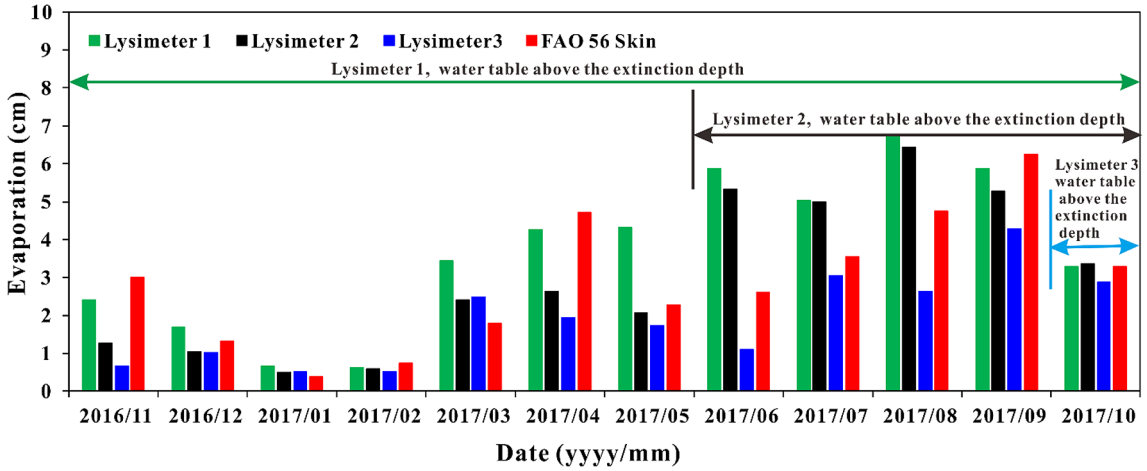

Fig. 7. Comparison of monthly evaporation rates based on the FAO-56 skin method with actual evaporation in lysimeter 1, lysimeter 2 and lysimeter 3. The extinction depth was 78 cm. The water table in lysimeter 1 was consistently above the extinction depth. In lysimeter 2, extinction depth was exceeded in the month of June. In lysimeter 3 the water table is above the extinction depth for a period of only 23 days (from October 9 to October 31, 2017).

Table 3
Comparison of FAO-56 skin method with actual evaporation. E_{fcum} is the cumulative evaporation from the FAO-56 skin method, E_{acum} is the cumulative actual evaporation. N_{over}, N_{under} indicate how many months the method over- or underestimated evaporation. We also indicate by how many % evaporation was over ($\%_{over}$) – or underestimated ($\%_{under}$) during these periods.

	Lysimeter 1	Lysimeter 2	Lysimeter 3
E_{fcum}/E_{acum} [%]	79	97	152
N_{over} [–]	5	6	10
($\%_{over}$)	9	42	64
N_{under} [–]	7	6	2
($\%_{under}$)	40	29	28

the FAO-56 skin method underestimated 21% of cumulative evaporation in lysimeter 1 (44.1 cm), and underestimated around 3% of cumulative evaporation in lysimeter 2 (35.8 cm), while overestimated 52% of cumulative evaporation in lysimeter 3 (22.7 cm). From November 2016 to May 2017, the FAO-56 skin method overestimated 36% of actual evaporation in lysimeter 2, and underestimated 19% evaporation after May. A more detailed overview of this comparison is compiled in Table 3. The cumulative evaporation rates over the entire period, as well as the number of months where evaporation was either over- or underestimated, as well as the % of under- and overestimation during these periods is shown.

3.5. Comparison with the actual evaporation and the results of the MEP method

The comparison between MEP and actual evaporation for lysimeter 1, lysimeter 2 and 3 are shown in Fig. 8. As opposed to the FAO-56 skin method (Fig. 7), the MEP results were closer to the actual evaporation for all lysimeters. On a annual scale, the result of MEP (41.5 cm) was close to the actual evaporation (44.1 cm) in lysimeter 1. MEP underestimated the annual actual evaporation by 6%. The cumulative evaporation of MEP was 35.5 cm in lysimeter 2, which is 99.2% of the actual evaporation (Table 4). The cumulative evaporation of MEP for lysimeter 3 was 26.1 cm, which was larger than the actual value of 22.7 cm. MEP overestimated the annual actual evaporation in lysimeter 3 by 14.8%. The very good performance on an annual basis is, however, related to the fact that some months are over- while other months are underestimated. Table 4 provides a detailed analysis of the monthly performance.

On a monthly scale, MEP overestimated evaporation for all lysimeters from April to July, especially during June and July. Besides that, MEP overestimated evaporation during August for lysimeter 3. Soil moisture content near the surface ground was still low in lysimeter 3 in August (the mean soil water content at 3 cm of the surface ground in August is 0.068 cm^3/cm^3). From November to January, March, and August to October, MEP underestimated evaporation for all lysimeters (except for August in lysimeter 3). In addition, our result showed that MEP underestimated evaporation when R_n was lowest from November to January.

3.6. Comparison of actual evaporation with the groundwater level fluctuation method

According to the pumping tests, the specific yields of the three lysimeters were 0.30, 0.31 and 0.30, the average value is 0.30. The second approach to estimate specific yield was based on Sophocleous (1991). The approach from Sophocleous results in estimates of the specific yield equaled to 0.12. The significant differences in the estimation of this crucial parameter are further discussed in section 4. The application of the GLF method requires declining water tables. As lysimeters 2 and 3 are, most of the time, below the extinction depth, the analysis must be limited to lysimeter 1.

Fig. 9 shows the results of the GLF. The GLF-G1 approach significantly overestimated actual evaporation every month, especially from March to October 2017 (Fig. 9). The cumulative evaporation based on the GLF-G1 was 140.6 cm. This implies that the GLF-G1 method significantly overestimated evaporation, by 227.0% for one year. Table 5 provides a detailed analysis of the monthly performance.

Compared with the GLF-G1 method, the GLF-G2 method yields more accurate results. On a monthly scale, the results of GLF-G2 were consistent with the actual evaporation, except for September and October 2017. The cumulative evaporation of GLF-G2 was 56.3 cm, as compared to 44.1 cm of actual evaporation. This implies that the GLF-G2 method was a reliable method for estimating evaporation from shallow water table depth.

3.7. Comparison of the actual evaporation with Darcy's law

The laboratory-based van Genuchten parameters do adequately represent the real field conditions. This could, for example, be related to hysteresis. The results (not shown) were not satisfactory as the fluxes are often negative, even during periods where no precipitation occurred. To explore to what extent this method can reproduce evaporation dynamics, we calibrated the soil parameters by minimizing the

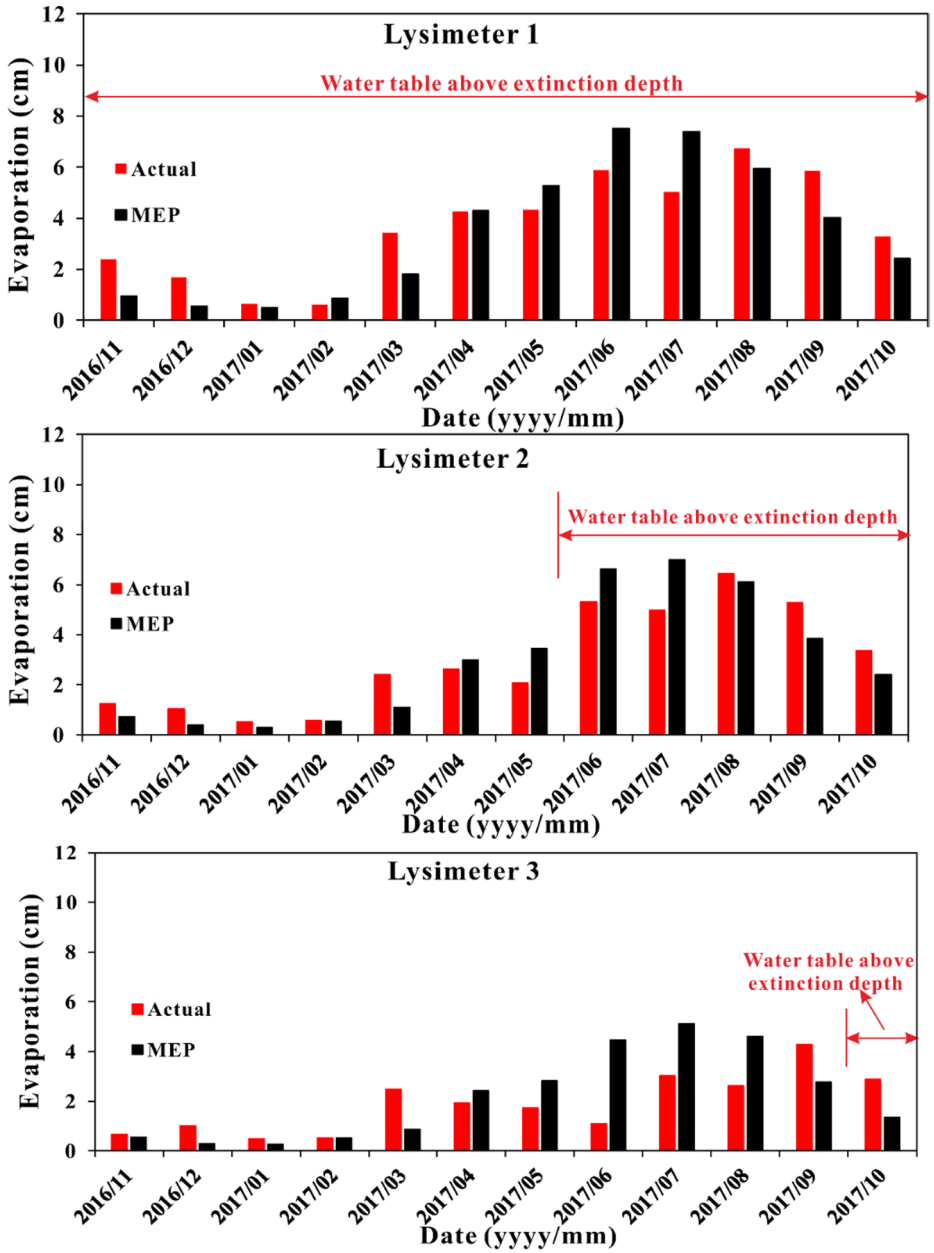

Fig. 8. Comparison between monthly evaporation rates based on MEP with actual evaporation in lysimeter 1 (a), lysimeter 2 (b) and lysimeter 3 (c). During the period from August to October, the amount of rainfall was 29.6 cm, which accounted for 47.6% of the annual rainfall during the experimental period.

Table 4
Comparison of the MEP method with actual evaporation. E_{Mcum} is the cumulative evaporation from the MEP method, E_{acum} is the cumulative actual evaporation. N_{over}, N_{under} indicate how many months the method over- or underestimated evaporation. We also indicate by how many % evaporation was over ($\%_{over}$) – or underestimated ($\%_{under}$) during these periods.

	Lysimeter 1	Lysimeter 2	Lysimeter 3
E_{Mcum}/E_{acum} [%]	94	99	115
N_{over} [–]	5	4	6
$\%_{over}$	26	34	83
N_{under} [–]	7	8	6
$\%_{under}$	33	26	48

difference between the observed and calculated evaporation rates. The calibrated parameters are shown in Table 6. The values of cumulative evaporation were 43.5, 34.6 and 24.1 cm for lysimeters 1, 2 and 3, respectively. The cumulative evaporation was very good for all three lysimeters. However, as opposed to lysimeter 1 and 2, lysimeter 3 had periods of over-and underestimation. Fig. 10 displays the cumulative evaporation based on Darcy's law.

4. Discussion

Multiple methods to estimate evaporation were compared and different implementations of several of these methods were tested. While several studies comparing different methods to estimate bare soil evaporation exist, we are not aware of a study comparing the different methods to accurate, lysimeter based measurements of actual evaporation.

An initial analysis of the meteorological and soil conditions showed that most of the time our system was not controlled by the atmosphere, but rather by soil water availability and the soil properties. This is a typical situation for arid-and semi-arid regions. Nevertheless, the experimental setup we chose allowed us to explore significantly different

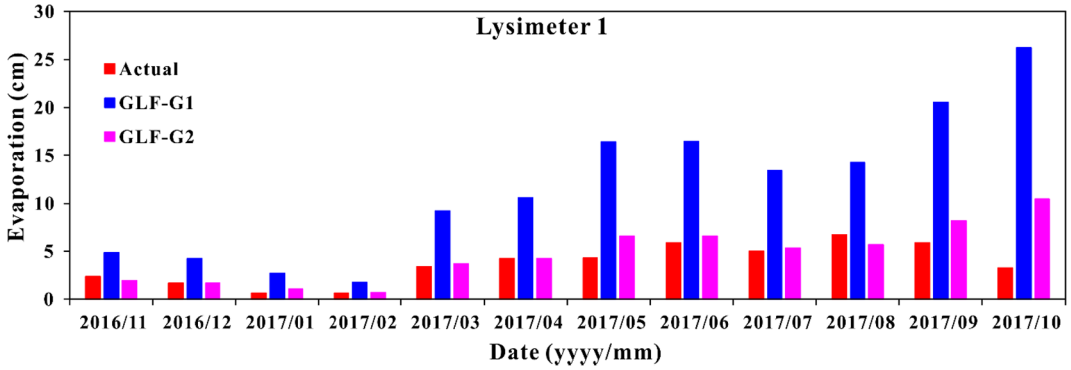

Fig. 9. Comparison of monthly evaporation rate using GLF-G1 and GLF-G2 in lysimeter 1. GLF-G1(specific yield obtained by pumping test) and GLF-G2 (specific yield obtained by the soil water balance).

Table 5
Comparison of GLF method with actual evaporation in lysimeter 1. E_{Gcum} is the cumulative evaporation from the GLF method, E_{acum} is the cumulative actual evaporation. N_{over}, N_{under} indicate how many months the method over- or underestimated evaporation. We also indicate by how many % evaporation was over ($\%_{over}$) – or underestimated ($\%_{under}$) during these periods.

	GLF-G1	GLF-G2
E_{Gcum}/E_{acum} [%]	319	127
N_{over} [–]	12	9
$\%_{over}$	219	44
N_{under} [–]	0	3
$\%_{under}$	0	11

Table 6
Calibrated parameters for Darcy's law. See Table 2 for a comparison with the laboratory-based values. The largest changes to the laboratory data are for α.

Lysimeter	θ_s [cm^3/cm^3]	θ_r [cm^3/cm^3]	α [cm^{-1}]	n [–]	K_S [cm/d]
1	0.32	0.02	0.09	1.43	450
2	0.32	0.01	0.06	2.22	450
3	0.32	0.01	0.01	1.66	450

hydrological conditions: owing to the instrumentation and different initial conditions of our lysimeters, our study could systematically explore the performance of the different methods in relation to the water table depth.

The extinction depth could be graphically identified, in this case it was 78 cm. If the water table is below this depth, no evaporation from groundwater takes place and all evaporation originates from rainfall. Lysimeter 1 was above the extinction depth throughout the experiment, therefore groundwater contributed to evaporation. In lysimeter 3, on the other hand, groundwater contributed only for the last 23 days of the experiment. Lysimeter 2 was between the two extremes, with 5 months below the extinction depth. As our lysimeters are disconnected from the regional groundwater table, the water table in these lysimeters cannot fall below this level. Lysimeters are therefore very well suited to identify the extinction depth for a given soil. However, a clear separation between the contribution of groundwater and rainfall to the total evaporation requires a more detailed analysis and it not the focus of this study.

Our data suggest that across one year and for all lysimeters, MEP performed significantly better than all other methods. Nevertheless, a monthly analysis suggests that MEP can over- or underestimate the evaporation significantly. Alves et al. (2019) pointed out that MEP tends to overestimate evaporation for dry soil conditions. In our study, the largest overestimation was observed for lysimeter 3 (306%) in June, a period coincides with very dry conditions. As opposed to the other two lysimeters, no capillary rise can contribute to evaporation. Our results confirm that MEP overestimates evaporation for dry conditions. The problem is accentuated if the water table is below the extinction depth: During the dry period of June and July, the overestimation of evaporation using MEP is less important in lysimeter 1 and 2 as compared to lysimeter 3. In lysimeters 1 and 2 the water table is above the extinction depth and thus can contribute to maintaining a certain level of soil moisture. This is an important insight as it allows us to identify periods where MEP overestimates evaporation rates. A way to improve the performance of MEP during dry conditions could be the direct measurement of specific humidity (q_s). In our study, we estimated the specific humidity using equation (22) and (23), but a direct measurement (for example using iButton Hydrochron sensors) might increase the reliability of the results.

For certain periods, MEP underestimates the evaporation rates. We could not identify a systematic relation between the water table being above or below the extinction depth and the underestimation of the evaporation rates. MEP underestimated evaporation rates during precipitation events.

In terms of overall performance, the FAO-56 skin method closely followed the MEP approach. As with the MEP method, the performance

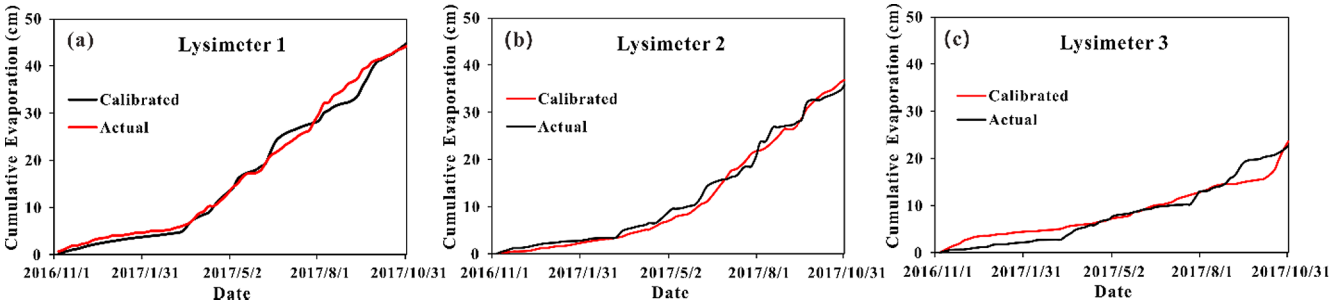

Fig. 10. Comparison of monthly evaporation rate using Darcy's law method in lysimeter 1 (a), lysimeter 2 (b) and lysimeter 3 (c). Calibrated means that the cumulative evaporation from Darcy's law method using calibrated parameters in Table 6, and actual means that actual cumulative evaporation.

of the FAO-56 skin method is dependant on the water table concerning the extinction depth. If the water table is above the extinction depth (as is the case for lysimeter 1 throughout the experiment period), the FAO-56 skin method tends to underestimate the evaporation rate. This is consistent with previous findings: Allen (2011) pointed out that the FAO-56 skin method underestimated the evaporation because of capillary rise is not taken into account. On the other hand, we found that if the water table is consistently below the extinction depth (as is the case for lysimeter 3), the FAO-56 method systematically overestimated the evaporation rate (except for 2 months which do not significantly affect the trend to overestimate evaporation). The good overall, cumulative performance of lysimeter 2 is related to the fact that the periods of over- and underestimation compensate each other. As pointed out by Allen et al. (2005), critical parameters in the application of the FAO-56 method are the REW, TEW and K_{emax}. The implementation of this method was based on the parameter values found in the literature. It is possible that adaption of the parameters to field-specific conditions could further improve the performance (Mutziger et al., 2005).

Although the method of groundwater level fluctuation is relatively simple to implement, falling water tables are required. This can be a limiting factor in arid-and semi-arid regions, where the water table is often below the extinction depth. Another issue is related to the estimation of the specific yield. The estimation of evaporation based on the specific yield obtained through a pumping test was not satisfactory as evaporation rates were overestimated significantly. However, the performance of this method increased significantly with our second estimate of the specific yield. The second method considered storage changes in the unsaturated zone, too, and is thus better suited for this kind of application. The estimation of specific yield will remain a problem for the application for this method. Estimating the specific yield is further complicated by effects such as plant growth (Logsdon et al., 2010), hysteresis (Nachabe, 2002), and initial water table depth (Cheng et al., 2020).

Darcy's law is a method to estimate evaporation using field observations of soil moisture. Conceptually, the application fo Darcy's law is straightforward. However, the problem is related to the parametrization of the soil–water characteristic curve. The application of the parameters obtained in the laboratory did not allow a sound estimation of the evaporation rates, even though a very good fit between pressure-head and soil moisture could be obtained. After the application of Darcy's law based on the laboratory parameters, we modified the soil retention parameters to reduce the mismatch between observed and calculated evaporation rates. For all lysimeters, a very good fit could be obtained with one set of parameters. This clearly suggests that conceptually Darcy's law remains a very interesting approach, provided the soil–water characteristic curve is known. This, however, will not be the case in most situations.

5. Conclusions

The study explored the performance of four commonly used methods to estimate evaporation in semi-arid conditions. Different implementations of the methods were analysed. We used experimental data of three lysimeters with different water table depths. Based on the experimental data from sandy soil under the semi-arid climate condition, the following conclusions/recommendations can be drawn:

(1) The MEP method provided the best results in all lysimeters. MEP overestimated evaporation for dry conditions. If the water table is below the extinction depth, the largest biases are expected.
(2) The FAO-56 skin method could generally obtain good results. The method tended to underestimate the evaporation when the water table was above the extinction depth and overestimated the evaporation when the water table depth was larger than the extinction depth. We recommend to determine the extinction depth and measure the water table for a first-order indication of the performance of this method.
(3) Two approaches for the water table fluctuations were employed: GLF-G1 significantly overestimated the evaporation, due to uncertainties of the specific yield obtained from the pumping test. GLF-G2, which used a soil water balance for a better estimation of the specific yield could reproduce the bare soil evaporation across all groundwater depths. However, the water balance method requires falling water tables, which is only the case if the groundwater level is above the extinction depth. If the water table is below the extinction depth, a falling water table cannot be associated with evaporation.
(4) We could show that Darcy's law is in principle capable of reproducing evaporation dynamics very well. The issue, however, is that the required parameters for the soil–water characteristic curve at often not known. The parameters obtained in the laboratory resulted in a significant mismatch between observed and estimated evaporation rates. This is a serious limitation of the method which will undermine its applicability in most of the cases.
(5) Given the importance of the extinction depth in many of these methods, we suggest that the extinction depth is analyzed and the water table is measured as an integral part of evaporation studies. It provides a useful point of reference for the performance of the MEP and FAO-56 skin method.
(6) Lysimeters were very well suited for this comparative analysis. We recommend the installation of lysimeters for areas where soil evaporation needs to be quantified. Ideally, weighing lysimeters are employed. Given the significant cost of such lysimeters, the soil-moisture balance based on soil moisture sensors is a pragmatic and useful alternative.

CRediT authorship contribution statement

Chengcheng Gong: Writing - original draft, Writing - review & editing, Data curation, Methodology. **Wenke Wang:** Funding acquisition, Resources, Writing - original draft. **Zaiyong Zhang:** Data curation, Methodology, Writing - original draft, Software. **Hao Wang:** Investigation, Data curation. **Jie Luo:** Investigation, Data curation. **Philip Brunner:** Writing - original draft, Writing - review & editing, Supervision, Methodology.

Declaration of Competing Interest

The authors declare that they have no known competing financial interests or personal relationships that could have appeared to influence the work reported in this paper.

Acknowledgments

This study was supported by the National Natural Science Foundation of China (No. U1603243, 41902249), the National Key Research and Development Program of China (No. 2018YFC0406504), and the Key Research and Development Program of Shaanxi (Program No. 2019SF05-01). The first author is grateful to Chang'an University Short-Term Study Abroad Program for Postgraduate Students (No.0021/300203110004) and Chinese Scholarship Council (No. 201906560022) for providing an opportunity to be a visiting student at the University of Neuchâtel. The analysis was also partially supported by the SAFEA: High-End Foreign Experts Project (No. G20190027031). We thank Prof. Jingfeng Wang for his suggestion and assistance in the MEP method. We are also very grateful to Prof. Richard G. Allen who gave us a lot of help in using the FAO-56 skin method. We are grateful for the insightful comments and constructive suggestions from three anonymous reviewers and editors.

References

Allen, R.G., 2011. Skin layer evaporation to account for small precipitation events—An enhancement to the FAO-56 evaporation model. Agric. Water Manag. 99 (1), 8–18.

Allen, R.G., Pereira, L.S., Raes, D., Smith, M., 1998. Crop evapotranspiration-Guidelines for computing crop water requirements-FAO Irrigation and drainage paper 56. Fao, Rome 300 (9), D05109.

Allen, R.G., Pruitt, W.O., Raes, D., Smith, M., Pereira, L.S., 2005. Estimating evaporation from bare soil and the crop coefficient for the initial period using common soils information. J. Irrig. Drain. Eng. 131 (1), 14–23.

Alves, M., Music, B., Nadeau, D., Anctil, F., 2019. Comparing the performance of the maximum entropy production model with a land surface scheme in simulating surface energy fluxes. J. Geophys. Res.: Atmos. 124 (6), 3279–3300.

Bittelli, M., Ventura, F., Campbell, G.S., Snyder, R.L., Gallegati, F., Pisa, P.R., 2008. Coupling of heat, water vapor, and liquid water fluxes to compute evaporation in bare soils. J. Hydrol. 362 (3–4), 191–205.

Bonan, G.B., 2008. Forests and climate change: forcings, feedbacks, and the climate benefits of forests. Science 320 (5882), 1444–1449.

Brandes, D., Wilcox, B.P. 2000. Evapotranspiration and soil moisture dynamics on a semiarid ponderosa pine hillslope 1. JAWRA J. Am. Water Resour. Assoc. 36(5), 965–974.

Brunner, Li, H., Kinzelbach, W., Li, W., 2007. Generating soil electrical conductivity maps at regional level by integrating measurements on the ground and remote sensing data. Int. J. Remote Sens. 28(15), 3341–3361.

Brunner, Li, H., Kinzelbach, W., Li, W., Dong, X., 2008. Extracting phreatic evaporation from remotely sensed maps of evapotranspiration. Water Resour. Res. 44(8).

Chen, L., Wang, W., Zhang, Z., Wang, Z., Wang, Q., Zhao, M., Gong, C., 2018. Estimation of bare soil evaporation for different depths of water table in the wind-blown sand area of the Ordos Basin, China. Hydrogeol. J. 26 (5), 1693–1704.

Cheng, D.-H., Li, Y., Chen, X., Wang, W.-K., Hou, G.-C., Wang, C.-L., 2013. Estimation of groundwater evaportranspiration using diurnal water table fluctuations in the Mu Us Desert, northern China. J. Hydrol. 490, 106–113.

Cheng, D., Wang, W., Zhan, H., Zhang, Z., Chen, L., 2020. Quantification of transient specific yield considering unsaturated-saturated flow. J. Hydrol. 580. https://doi.org/10.1016/j.jhydrol.2019.124043.

Chinnasamy, P., Maheshwari, B., Dillon, P., Purohit, R., Dashora, Y., Soni, P., Dashora, R., 2018. Estimation of specific yield using water table fluctuations and cropped area in a hardrock aquifer system of Rajasthan, India. Agric. Water Manag. 202, 146–155.

Cobos, D.R., Chambers, C., 2010. Calibrating ECH2O soil moisture sensors. Appl. note 1–5.

Cooper, J., Gardner, C., Mackenzie, N., 1990. Soil controls on recharge to aquifers. J. Soil Sci. 41 (4), 613–630.

Crosbie, R.S., Binning, P., Kalma, J.D., 2005. A time series approach to inferring groundwater recharge using the water table fluctuation method. Water Resour. Res. 41 (1).

Davarzani, H., Smits, K., Tolene, R.M., Illangasekare, T., 2014. Study of the effect of wind speed on evaporation from soil through integrated modeling of the atmospheric boundary layer and shallow subsurface. Water Resour. Res. 50 (1), 661–680.

Dewar, R.C., 2005. Maximum entropy production and the fluctuation theorem. J. Phys. A: Math. Gen. 38 (21), L371.

Deardorff, J.W., 1977. A parameterization of ground-surface moisture content for use in atmospheric prediction models. J. Appl. Meteorol. 16 (11), 1182–1185.

Flammini, A., Corradini, C., Morbidelli, R., Saltalippi, C., Picciafuoco, T., Giráldez, J.V., 2018. Experimental analyses of the evaporation dynamics in bare soils under natural conditions. Water Resour. Manage. 32 (3), 1153–1166.

Freeze, R.A., Cherry, J.A. 1979. Groundwater, vol. 176. Prentice-hall, Englewood Cliffs, NJ, pp. 161–177.

Gao, H., Cai, X., He, H., 2009. The Impact of Urbanization on the Surface Temperature in Xi'an. Acta Geog. Sin. 64 (9), 1093–1102.

Gardner, W., 1958. Some steady-state solutions of the unsaturated moisture flow equation with application to evaporation from a water table. Soil Sci. 85 (4), 228–232.

Gardner, W., Fireman, M., 1958. Laboratory studies of evaporation from soil columns in the presence of a water table. Soil Sci. 85 (5), 244–249.

Hajji, I., Nadeau, D.F., Music, B., Anctil, F., Wang, J., 2018. Application of the maximum entropy production model of evapotranspiration over partially vegetated water-limited land surfaces. J. Hydrometeorol. 19 (6), 989–1005.

Hellwig, D., 1973. Evaporation of water from sand, 1: Experimental set-up and climatic influences. J. Hydrol. 18 (2), 93–108.

Hellwig, D., 1973. Evaporation of water from sand, 4: The influence of the depth of the water-table and the particle size distribution of the sand. J. Hydrol. 18 (3–4), 317–327.

Henderson-Sellers, A., Irannejad, P., McGuffie, K., Pitman, A., 2003. Predicting land-surface climates-better skill or moving targets? Geophys. Res. Lett. 30 (14).

Hill, A.J., Durchholz, B., 2015. Specific yield functions for estimating evapotranspiration from diurnal surface water cycles. JAWRA J. Am. Water Resour. Assoc. 51 (1), 123–132.

Huang, S.Y., Wang, J., 2016. A coupled force-restore model of surface temperature and soil moisture using the maximum entropy production model of heat fluxes. J. Geophys. Res.: Atmos. 121 (13), 7528–7547.

Kinzelbach, W., Bauer, P., Siegfried, T., Brunner, P. 2003. Sustainable groundwater management–Problems and scientific tool. Episodes-Newsmag. Int. Union Geol. Sci. 26(4), 279–284.

Kornejady, A., Ownegh, M., Bahremand, A., 2017. Landslide susceptibility assessment using maximum entropy model with two different data sampling methods. Catena 152, 144–162.

Lautz, L.K., 2008. Estimating groundwater evapotranspiration rates using diurnal water-table fluctuations in a semi-arid riparian zone. Hydrogeol. J. 16 (3), 483–497.

Lawrence, D.M., Thornton, P.E., Oleson, K.W., Bonan, G.B. 2007. The partitioning of evapotranspiration into transpiration, soil evaporation, and canopy evaporation in a GCM: Impacts on land–atmosphere interaction. J. Hydrometeorol. 8(4), 862–880.

Lehmann, P., Assouline, S., Or, D. 2008. Characteristic lengths affecting evaporative drying of porous media. Phys. Rev. E, 77(5), 056309.

Li, H., Brunner, P., Kinzelbach, W., Li, W., Dong, X., 2009. Calibration of a groundwater model using pattern information from remote sensing data. J. Hydrol. 377 (1–2), 120–130.

Li, H., Kinzelbach, W., Brunner, P., Li, W., Dong, X., 2008. Topography representation methods for improving evaporation simulation in groundwater modeling. J. Hydrol. 356 (1–2), 199–208.

Li, N., Zhao, P., Wang, J., Deng, Y., 2020. The long-term change of latent heat flux over the Western Tibetan Plateau. Atmosphere 11 (3). https://doi.org/10.3390/atmos11030262.

Liu, X., Xu, C., Zhong, X., Li, Y., Yuan, X., Cao, J., 2017. Comparison of 16 models for reference crop evapotranspiration against weighing lysimeter measurement. Agric. Water Manage. 184, 145–155.

Logsdon, S., Schilling, K., Hernandez-Ramirez, G., Prueger, J., Hatfield, J., Sauer, T., 2010. Field estimation of specific yield in a central Iowa crop field. Hydrol. Processes: Int. J. 24 (10), 1369–1377.

Loheide, S.P., 2008. A method for estimating subdaily evapotranspiration of shallow groundwater using diurnal water table fluctuations. Ecohydrol.: Ecosyst. Land Water Process Interactions Ecohydrogeomorphol. 1 (1), 59–66.

Loheide, S.P., Butler Jr, J.J., Gorelick, S.M., 2005. Estimation of groundwater consumption by phreatophytes using diurnal water table fluctuations: a saturated-unsaturated flow assessment. Water Resour. Res. 41 (7).

Ministry of Water Resources of China (MWR) (2010), China water resources bulletin, Ministry of Water Resources of China, Beijing. [Available at http://www.mwr.gov.cn/].

Mualem, Y., 1976. A new model for predicting the hydraulic conductivity of unsaturated porous media. Water Resour. Res. 12 (3), 513–522.

Mutziger, A.J., Burt, C.M., Howes, D.J., Allen, R.G., 2005. Comparison of measured and FAO-56 modeled evaporation from bare soil. J. Irrig. Drain. Eng. 131 (1), 59–72.

Nachabe, M.H., 2002. Analytical expressions for transient specific yield and shallow water table drainage. Water Resour. Res. 38 (10), 11-1-11-7.

Qiao, G., Wang, W., 2014. Evaporation intensity of bare soil in a northwest arid inland basin. J. Jilin Univ. (Earth Sci. Ed.) 44 (4), 1327–1332.

Quinn, R., Parker, A., Rushton, K., 2018. Evaporation from bare soil: Lysimeter experiments in sand dams interpreted using conceptual and numerical models. J. Hydrol. 564, 909–915.

Rianna, G., Reder, A., Pagano, L., 2018. Estimating actual and potential bare soil evaporation from silty pyroclastic soils: Towards improved landslide prediction. J. Hydrol. 562, 193–209.

Ritchie, J., Johson, B. 1990. Soil and plant factors affecting evaporation. Agronomy (30), 363–390.

Saito, H., Šimůnek, J., Mohanty, B.P., 2006. Numerical analysis of coupled water, vapor, and heat transport in the vadose zone. Vadose Zone J. 5 (2), 784–800.

Salvucci, G.D., 1993. An approximate solution for steady vertical flux of moisture through an unsaturated homogeneous soil. Water Resour. Res. 29 (11), 3749–3753.

Shah, N., Ross, M., 2009. Variability in specific yield under shallow water table conditions. J. Hydrol. Eng. 14 (12), 1290–1298.

Shahraeeni, E., Lehmann, P., Or, D., 2012. Coupling of evaporative fluxes from drying porous surfaces with air boundary layer: Characteristics of evaporation from discrete pores. Water Resour. Res. 48 (9).

Shanafield, M., Cook, P.G., Gutiérrez-Jurado, H.A., Faux, R., Cleverly, J., Eamus, D., 2015. Field comparison of methods for estimating groundwater discharge by evaporation and evapotranspiration in an arid-zone playa. J. Hydrol. 527, 1073–1083.

Shih, S.F., 1983. Soil surface evaporation and water table depths. J. Irrig. Drainage Eng. 109(4), 366–376.

Shokri, N., Lehmann, P., Vontobel, P., Or, D. 2008. Drying front and water content dynamics during evaporation from sand delineated by neutron radiography. Water Resour. Res. 44(6).

Shokri, N., Salvucci, G., 2011. Evaporation from porous media in the presence of a water table. Vadose Zone J. 10 (4), 1309–1318.

Smits, K.M., Ngo, V.V., Cihan, A., Sakaki, T., Illangasekare, T.H., 2012. An evaluation of models of bare soil evaporation formulated with different land surface boundary conditions and assumptions. Water Resour. Res. 48 (12).

Sophocleous, M.A., 1991. Combining the soilwater balance and water-level fluctuation methods to estimate natural groundwater recharge: practical aspects. J. Hydrol. 124 (3–4), 229–241.

Stephens, D.B., Knowlton Jr., R., 1986. Soil water movement and recharge through sand at a semiarid site in New Mexico. Water Resour. Res. 22 (6), 881–889.

Suleiman, A.A., Soler, C.M.T., Hoogenboom, G., 2007. Evaluation of FAO-56 crop coefficient procedures for deficit irrigation management of cotton in a humid climate. Agric. Water Manag. 91 (1–3), 33–42.

Tran, D.T., Fredlund, D.G., Chan, D.H. 2015. Improvements to the calculation of actual evaporation from bare soil surfaces. Can. Geotechn. J. 53(1), 118–133.

Trautz, A.C., Smits, K.M., Cihan, A., 2015. Continuum-scale investigation of evaporation from bare soil under different boundary and initial conditions: an evaluation of nonequilibrium phase change. Water Resour. Res. 51 (9), 7630–7648.

Valipour, M., Sefidkouhi, M.A.G., Raeini, M., 2017. Selecting the best model to estimate potential evapotranspiration with respect to climate change and magnitudes of extreme events. Agric. Water Manage. 180, 50–60.

Van Genuchten, M.T., 1980. A closed-form equation for predicting the hydraulic

conductivity of unsaturated soils 1. Soil Sci. Soc. Am. J. 44 (5), 892–898.
Veihmeyer, F., Brooks, F., 1954. Measurements of cumulative evaporation from bare soil. Eos, Trans. Am. Geophys. Union 35 (4), 601–607.
Wang, J., Bras, R., 2011. A model of evapotranspiration based on the theory of maximum entropy production. Water Resour. Res. 47 (3).
Wang, W., Zhang, Z., Duan, L., Wang, Z., Zhao, Y., Zhang, Q., Dai, M., Liu, H., Zheng, X., Sun, Y., 2018. Response of the groundwater system in the Guanzhong Basin (central China) to climate change and human activities. Hydrogeol. J. 26 (5), 1429–1441.
Wang, W., Zhang, Z., Yeh, T.-c.J., Qiao, G., Wang, W., Duan, L., Huang, S.-Y., Wen, J.-C. 2017. Flow dynamics in vadose zones with and without vegetation in an arid region. Adv. Water Resour. 106, 68–79.
Wang, W., Zhao, G., Li, J., Hou, L., Li, Y., Yang, F., 2011. Experimental and numerical study of coupled flow and heat transport. In: Proceedings of the Institution of Civil Engineers-Water Management. Thomas Telford Ltd, pp. 533–547.
Yang, Y., Yang, Y., Moiwo, J.P., Hu, Y., 2010. Estimation of irrigation requirement for sustainable water resources reallocation in North China. Agric. Water Manage. 97 (11), 1711–1721.
Zhang, Z., Wang, W., Gong, C., Wang, Z., Duan, L., Yeh, T.c.J., Yu, P. 2019. Evaporation from seasonally frozen bare and vegetated ground at various groundwater table depths in the Ordos Basin, Northwest China. Hydrol. Processes, 33(9), 1338–1348.
Zhang, Z., Wang, W., Wang, Z., Chen, L., Gong, C., 2018. Evaporation from bare ground with different water-table depths based on an in-situ experiment in Ordos Plateau, China. Hydrogeol. J. 26 (5), 1683–1691.
Zuo, D., Xu, Z., Cheng, L., Liu, X., 2011. Spatial-temporal variations and mutations of potential evapotranspiration in the Weihe river basin. Resour. Sci. 33 (5), 975–982.